

Floquet Nonadiabatic Nuclear Dynamics with Photoinduced Lorenz-Like Force in Quantum Transport

Jingqi Chen,^{1, 2, 3} Wei Liu,^{2, 3} and Wenjie Dou^{2, 3, *}

¹*Fudan University, Shanghai 200433, China*

²*School of Science, Westlake University, Hangzhou, Zhejiang 310024, China*

³*Institute of Natural Sciences, Westlake Institute for Advanced Study, Hangzhou, Zhejiang 310024, China*

In our recent paper [Mosallanejad *et al.*, Phys. Rev. B 107(18), 184314, 2023], we have derived a Floquet electronic friction model to describe nonadiabatic molecular dynamics near metal surfaces in the presence of periodic driving. In this work, we demonstrate that Floquet driving can introduce an anti-symmetric electronic friction tensor in quantum transport, resulting in circular motion of the nuclei in the long time limit. Furthermore, we show that such a Lorenz-like force strongly affects nuclear motion: at lower voltage bias, Floquet driving can increase the temperature of nuclei; at larger voltage bias, Floquet driving can decrease the temperature of nuclei. In addition, Floquet driving can affect electron transport strenuously. Finally, we show that there is an optimal frequency that maximizes electron current. We expect that the Floquet electronic friction model is a powerful tool to study nonadiabatic molecular dynamics near metal surfaces under Floquet driving in complex systems.

PACS numbers:

INTRODUCTION

The Born-Oppenheimer approximation has long stood as a pillar in quantum chemistry, offering a powerful framework to decouple electronic and nuclear motions in molecular systems. However, its applicability wanes when confronted with scenarios where nuclei interact nonadiabatically with a manifold of electronic states. One such intriguing instance arises in systems like adsorbates on metal surfaces, where the conventional Born-Oppenheimer separation of electronic and nuclear degrees of freedom becomes inadequate [1–3]. The complexity of these interactions demands a more nuanced approach, leading to the emergence of the electronic friction (EF) model. The EF model represents a compelling paradigm shift in our understanding of nonadiabatic dynamics near metal surfaces [4–9]. Unlike the Born-Oppenheimer approximation, which relies on a strict separation of timescales, the EF model acknowledges the intricate interplay between electrons and nuclei in a dynamically evolving environment. This model goes beyond the realm of traditional theoretical frameworks, accounting for the frictional forces that electrons experience as they navigate through a medium. In doing so, it captures the effects of both friction and random forces arising from the surrounding bath of particles, providing a comprehensive picture of nonadiabatic interactions.

Within the EF model, a notable distinction arises in the treatment of the friction tensor. This tensor, a key concept in the theory, encompasses both symmetric and anti-symmetric components. While the symmetric part has traditionally dominated discussions due to its prevalence in many systems, recent research has unveiled the significance of the anti-symmetric sector. While often considered negligible or even assumed to be zero, certain

intriguing scenarios challenge this assumption. These situations give rise to a non-zero Berry curvature within the electronic friction tensor, leading to the emergence of a novel force—the Berry force [10, 11]. The Berry force stands as a tantalizing frontier in the study of nonadiabatic dynamics. It introduces a new layer of complexity and richness to our understanding of molecular behavior near metal surfaces and other systems characterized by strong nonadiabatic interactions. Incorporating the Berry force into the EF model offers an unprecedented opportunity to delve into the intricate coupling between electronic and nuclear degrees of freedom. As a result, researchers are empowered to shed light on the dynamics of adsorbates on metal surfaces and explore a wide array of complex systems, paving the way for new insights and breakthroughs in the realm of nonadiabatic interactions.

Previous studies have shown that the friction tensor can exhibit anti-symmetric terms in two situations. Firstly, Lu *et al.* [10, 12] found that a steady direct current or the presence of two leads with different Fermi levels (out of equilibrium) can make the anti-symmetric friction tensor non-zero, leading to a current-induced Berry force. Secondly, Subotnik *et al.* [13] showed that spin-orbital couplings (SOC) or complex Hamiltonians can also lead to a Lorenz-like Berry force even at equilibrium [11, 14]. The Berry force arising from SOC is referred to as the spin Berry force. In both cases, the anti-symmetric part of the electronic friction tensor can contribute to a Lorenz-like Berry force. It was also noted that there is an important connection between the Berry force and nonadiabatic dynamics.

Our recent study [15] investigated the photoinduced Lorenz-like Berry force using the Floquet theory, where we considered light as a periodic driving. We formulated a QCLE in Floquet representation to describe nonadi-

abatic dynamics with light-matter interactions (LMIs). We then mapped Floquet QCLE to the EF model and found that the anti-symmetric friction tensor is no longer zero after introducing light without bias, demonstrating that LMIs can independently give molecular junctions a Lorenz-like Berry curvature force. Actually, the LMIs break time-reversal symmetry, generating a Berry curvature force similar to that of a magnetic field, which can lead to the photo-induced quantum Hall effect [16–20]. Moreover, the anti-symmetric friction is larger than the symmetric one when the interaction between light and the system is relatively large, contributing to the dissipative process. Therefore, the effects of the photo-induced Berry force cannot be underestimated, but nobody has done such research before. Understanding how light-induced Berry curvature affects nonadiabatic dynamics is also the remaining question from our previous work, which will be beneficial for photo-chemistry [21–26].

Besides, the coexistence of current-induced Berry force and light-induced Berry force and their influence on nonadiabatic dynamics are not well understood. Specifically, it is unclear whether the effects of the two Lorenz-like forces add up or cancel each other out. Our research has significant implications for guiding photochemical reactions and understanding their underlying mechanisms.

In this paper, we study the joint influence of LMIs and bias on Berry force, and their influence on the nonadiabatic dynamical results (including the final kinetic energy and localized current). We organize this article as follows: in Sec. II, we describe our two-level model Hamiltonian and the Floquet EF model via non-equilibrium Green's functions near the metal surface; in Sec. III, we numerically present the anti-symmetric friction tensor, phonon relaxation dynamics, and localized current under different periodic drivings and biases; and we conclude and give the outlook in Sec. IV.

THEORY

A. Model Hamiltonian

We consider a general Hamiltonian to describe the quantum transport of a molecular junction. The total Hamiltonian can be described as an electronic Hamiltonian plus the nuclear kinetic energy:

$$\hat{H}_{tot} = \hat{H}_{el} + \sum_{\mu} \frac{P_{\mu}^2}{2M_{\mu}}. \quad (1)$$

The subscript μ indicates the nuclear degree of freedom (DoF). The electronic Hamiltonian \hat{H}_{el} can be separated into three parts: the molecule \hat{H}_s , the leads \hat{H}_b , and the

interactions between them \hat{H}_c :

$$\hat{H}_{el} = \hat{H}_s + \hat{H}_b + \hat{H}_c, \quad (2)$$

$$\hat{H}_s = \sum_{ij} [h_s]_{ij}(\mathbf{R}, t) \hat{d}_i^{\dagger} \hat{d}_j + U(\mathbf{R}), \quad (3)$$

$$\hat{H}_b = \sum_{\zeta k} \epsilon_{\zeta k} \hat{c}_{k\zeta}^{\dagger} \hat{c}_{k\zeta}, \quad (4)$$

$$\hat{H}_c = \sum_{\zeta k, i} V_{\zeta k, i} (\hat{c}_{k\zeta}^{\dagger} \hat{d}_i + \hat{d}_i^{\dagger} \hat{c}_{k\zeta}). \quad (5)$$

Here, \hat{d}_j and $\hat{c}_{k\zeta}$ are annihilation operators for the level in the molecule and the leads, respectively. $U(\mathbf{R})$ is the bare potential for the nuclei. We use $\zeta = L, R$ to denote left and right leads, and define the hybridization function $\Gamma_{\zeta ij}(\epsilon) = \sum_k V_{\zeta k, i} V_{\zeta k, j} \delta(\epsilon - \epsilon_{\zeta k})$ to characterize the system-bath couplings.

Note that we have introduced light-matter interactions (LMIs) in the system Hamiltonian $\mathbf{h}_s(\mathbf{R}, t)$. Here, we treat the light as a classical, time-dependent external field that couples to the system, such that the system Hamiltonian is time-periodic: $\mathbf{h}_s(\mathbf{R}, t + T) = \mathbf{h}_s(\mathbf{R}, t)$. Without loss of generality, we consider a two-level model with two-nuclear DoFs:

$$\mathbf{h}_s(\mathbf{R}, t) = \begin{pmatrix} x + \Delta & y + A \cos(\omega t) \\ y + A \cos(\omega t) & -x - \Delta \end{pmatrix}, \quad (6)$$

where x and y are nuclear DoFs. Δ on the diagonal part of the Hamiltonian is the energy difference between the two levels, in analogy to the driving force in the case of the two shifted parabolas. The off-diagonal terms of the Hamiltonian indicate the couplings between the two levels, which consist of nuclear couplings y as well as LMIs $A \cos(\omega t)$. $A \cos(\omega t)$ is a semi-classical representation of LMIs: A represents the strength of the interaction and ω is the frequency of the light. A schematic figure for our model Hamiltonian is shown in Fig. 1. In addition, we have set the bare nuclear potential $U(\mathbf{R})$ to be a two-dimensional harmonic oscillator:

$$U(\mathbf{R}) = \frac{1}{2} x^2 + \lambda_x x + \frac{1}{2} y^2 + \lambda_y y, \quad (7)$$

where we have chosen the frequencies of a two-dimensional harmonic oscillator to be 1 in both x and y directions. λ_x and λ_y shift the center of the Harmonic oscillator. As will be shown below, the bare potential does not affect the electronic friction but can change the dynamics overall.

B. Floquet EF model: adiabatic force, friction tensors, and random force

Utilizing the Floquet EF friction model, a semi-classical approach, we address the intricate dynamics of the system described in the previous subsection. The EF

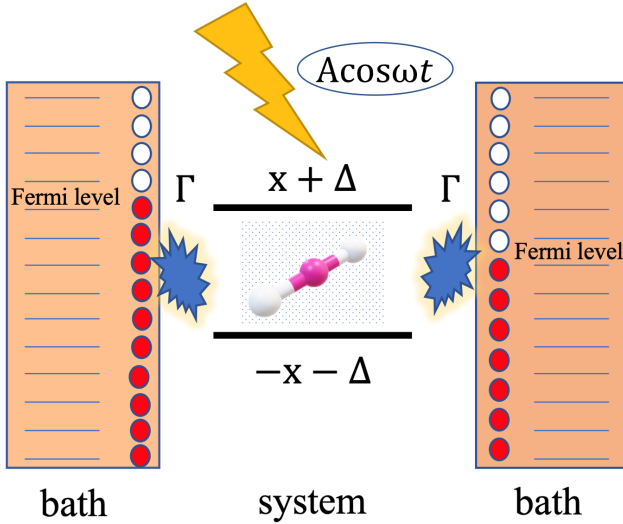


FIG. 1: A schematic picture for the model Hamiltonian: a two-level molecular junction is coupled with two baths (leads) with different Fermi levels. The light is only coupled with the system, not the baths.

model is valid when the timescales of the electrons and lights are faster than the nuclear motion. Such that we can trace out all electronic DoFs with LMIs. The resulting equation of motion for the nuclei is a Langevin equation:

$$M_\mu \ddot{R}_\mu = F_\mu^F - \sum_\nu \gamma_{\mu\nu}^F \dot{R}_\nu + \delta F_\mu^F. \quad (8)$$

Here μ and ν indicate nuclear DoFs, while M and R represent nuclear mass and position correspondingly. As for the three terms in the right hand side, F_μ^F is the mean force (adiabatic force), $\gamma_{\mu\nu}^F$ is the friction tensor (damping force), and δF_μ^F denotes a Markovian random force. The frictional and random forces represent the first-order correction to the Born-Oppenheimer approximation, i.e., the cooperated electron and light states are faster than the nuclear motion [6, 27].

Specifically, the adiabatic force, friction tensor, and

correlation function of the random force are given by:

$$\begin{aligned} \gamma_{\mu\nu}^F &= -\frac{\hbar}{2\pi(2N+1)} \times \\ &\int_{-\infty}^{+\infty} d\epsilon \text{Tr} \{ \partial_\mu h_s^F \partial_\epsilon G_r^F \partial_\nu h_s^F G_{<}^F \} + H.c., \\ F_\mu^F &= -\frac{1}{2\pi i(2N+1)} \times \\ &\int_{-\infty}^{+\infty} d\epsilon \text{Tr} \{ \partial_\mu h_s^F G_{<}^F \} - \partial_\mu U, \\ \frac{1}{2}(D_{\mu\nu}^F + D_{\nu\mu}^F) &= \frac{\hbar}{4\pi(2N+1)} \times \\ &\int_{-\infty}^{+\infty} d\epsilon \text{Tr} \{ \partial_\mu h_s^F G_{>}^F \partial_\nu h_s^F G_{<}^F \}. \end{aligned} \quad (9)$$

Here, Tr denotes trace over all electronic levels as well as Floquet levels. n denotes the Floquet level ($n = -N \dots N$), such that we have $2N+1$ total Floquet states. h_s^F is the Floquet representation of the system Hamiltonian:

$$h_s^F = \sum_{n=-N}^N h_s^{(n)} \hat{L}_n + \hat{N} \otimes \hat{I}_n \hbar\omega, \quad (10)$$

$$h_s^{(n)} = \frac{1}{T} \int_0^T h_s(R, t) e^{-in\omega t} dt, \quad (11)$$

where \hat{L}_n and \hat{N} are the ladder and number operators of the Floquet space. \hat{I}_n is the identity operator of the Floquet space. G_r^F , G_a^F , $G_{<}^F$, and $G_{>}^F$ are the retarded, advanced, lesser, and larger Floquet Green's functions of the electron in the energy domain, respectively. The Floquet Green's functions are given by:

$$\begin{aligned} G_r^F(\epsilon) &= (\epsilon - h_s^F - \Sigma_r^F)^{-1}, \\ G_a^F(\epsilon) &= G_r^F(\epsilon)^\dagger, \\ G_{<,>}^F(\epsilon) &= G_r^F(\epsilon) \Sigma_{<,>}^F(\epsilon) G_a^F(\epsilon). \end{aligned} \quad (12)$$

Here Σ_r^F is the retarded self-energy in Floquet space: $\Sigma_r^F = \Sigma_r \otimes \hat{I}_n$. We will apply the wide-band approximation such that $[\Sigma_r]_{ij} = -\frac{i}{2} \sum_\zeta \Gamma_{\zeta ij}$. $\Sigma_{<}^F$ (and $\Sigma_{>}^F$) is the lesser (and greater) self-energy in the Floquet space: $\Sigma_{<}^F = \sum_\zeta \Sigma_{\zeta <}^F$, where $[\Sigma_{\zeta <}^F]_{ij} = -i \Gamma_{\zeta ij} \otimes f(\epsilon - \hat{N} \hbar\omega - \mu_\zeta)$.

There are two levels in our model. We set orbital 1 couples to the left lead and orbital 2 couples to the right lead. Therefore, we can express the Γ matrix as:

$$\Gamma_L = \begin{pmatrix} \tilde{\Gamma} & 0 \\ 0 & 0 \end{pmatrix}, \quad \Gamma_R = \begin{pmatrix} 0 & 0 \\ 0 & \tilde{\Gamma} \end{pmatrix}. \quad (13)$$

Here, $\tilde{\Gamma}$ is a constant within the wide-band approximation. We can define the hybridization function in the Floquet space as $\Gamma_L^F = \Gamma_L \otimes \hat{I}_n$ and similarly $\Gamma_R^F = \Gamma_R \otimes \hat{I}_n$.

Note that the friction tensor is not necessarily symmetric. In Ref. [15], we show that when introducing periodical driving, $(\gamma^F$ exhibits anti-symmetric part, which

corresponds to a Lorentz-like force even at equilibrium (i.e., no electron voltage). Out of equilibrium, electron voltage can also introduce Lorentz-like forces. We expect the interplay of periodic driving and electronic voltage to give rise to an asymmetric friction tensor.

We get two random forces in both x and y directions relying on the correlation function of the random force $D_{\mu\nu}^F$, which is symmetric and positive-definite [6, 11]:

$$D^F = \begin{pmatrix} D_{xx}^F & D_{xy}^F \\ D_{yx}^F & D_{yy}^F \end{pmatrix}. \quad (14)$$

In our simulation, we generate two random numbers with a Gaussian distribution with norms $\sigma_\mu = \sqrt{2\tilde{D}_\mu^F/dt}$. Here \tilde{D}^F is the eigenvalue of the correlation function D^F . We then calculate the random force δF_μ^F by transforming the random numbers into the x and y basis.

C. Evaluating electron current

The total electron current is given by the integration of the local current over the phase space. In general, the local current with periodic driving is given by the Floquet Landauer formula [28–30]:

$$I_{loc}^F = \frac{e}{2\pi\hbar(2N+1)} \times \int_{-\infty}^{+\infty} d\epsilon \text{Tr} \{ T_{LR}^F(\epsilon) f_R^F(\epsilon) - T_{RL}^F(\epsilon) f_L^F(\epsilon) \}. \quad (15)$$

Notice that the transmission probabilities are not necessarily equal to each other, $T_{LR}^F \neq T_{RL}^F$. For our symmetric coupling case, we can further simplify the formula:

$$I_{loc}^F = \frac{e}{2\pi\hbar(2N+1)} \times \int_{-\infty}^{+\infty} d\epsilon \text{Tr} \{ T^F(\epsilon) [f_L^F(\epsilon) - f_R^F(\epsilon)] \}, \quad (16)$$

where $f_L^F(\epsilon)$ and $f_R^F(\epsilon)$ are the Floquet Fermi-Dirac distributions for the left and right leads, and $T^F(\epsilon)$ is the Floquet transmission probability that can be expressed in terms of Green's functions:

$$T^F(\epsilon) = \Gamma_L^F G_r^F(\epsilon) \Gamma_R^F G_a^F(\epsilon). \quad (17)$$

RESULTS AND DISCUSSIONS

A. Anti-symmetric friction tensor

We first plot the anti-symmetric friction tensor as a function of the nuclear coordinates (x, y) in Fig. 2 for different driving frequencies and driving amplitudes. As mentioned above, in the absence of periodic driving

and electron voltage, the friction tensor is symmetric and positive-definite. With periodic driving, the anti-symmetric part of the friction tensor exhibits peaks and dips in real space. As can be seen from each column of the figure, when increasing the bias, the shape of the anti-symmetric friction tensor does not change significantly, while the amplitude of the friction tensor increases with bias. When we increase the driving amplitude, we see more peaks and dips, as shown in the figures. This is because when we have strong LMIs, more Floquet replicas are coupled in. The overlaps of the Floquet replicas give rise to peaks and/or dips in the friction tensor. The positions of the peaks and dips are also very relevant to the driving frequency, as the driving frequency is related to the distance between the Floquet replicas.

To illustrate the effects of the Lorentz-like force on the dynamics, we also plot the steady-state distribution of the trajectories in the same plots. Here, we disregard the random force in Langevin dynamics. Notice that the trajectories enter a cycle limit due to the Lorentz force. In general, with a large bias, we have a strong Lorentz-like force, such that the radius of the cycle is larger. The position of the circle is mainly determined by the mean force, which does not change significantly with the driving frequency and amplitude. The driving frequency and amplitude affect the nuclear distribution stringently, highlighting the importance of the Floquet modulation on nuclear dynamics.

B. Langevin dynamics

We now run the full Floquet Langevin dynamics with the fluctuating force, and plot the observable in the long time limit (cycle limit). In particular, we are interested in the kinetic energy as well as the electron current.

In Fig. 3, we plot the kinetic energy for the nuclei in the cycle limit for different voltage biases and driving amplitudes and frequencies. Remarkably, when the bias is 0 and without any external driving ($A = 0$), the total kinetic energy is equal to kT , which constitutes the equilibrium kinetic energy baseline. However, upon introducing an external driving ($A \neq 0$), the total kinetic energy surpasses the kT threshold, indicating the emergence of heating effects induced by the external driving. Furthermore, our observations reveal that the parameter A , whether set at +1 or -1, does not exert any discernible influence on the kinetic energy. This suggests that, within the context of our system, the direction of the incident light does not alter the thermal consequences. Particularly, a more substantial driving amplitude corresponds to intensified heating. Notice that the Lorentz force preserves the kinetic energy unchanged, while the second fluctuation and dissipation theorem becomes inapplicable in the presence of Floquet driving.

Voltage bias can also introduce heating effects. That

being said, the combined presence of Floquet driving and voltage bias doesn't invariably result in intensified heating effects. Rather, at a larger bias (e.g., $\mu_L = 4$), the presence of the Floquet driving can diminish the heating effects. Conversely, external driving will most likely heat up the nuclei at low voltage bias.

Subsequently, we plot the total electron current under varying driving amplitudes and driving frequencies in Fig. 4. Note that without external driving, a larger bias can lead to a current profile exhibiting negative resistance characteristics. Such a phenomenon stems from nuclear motion. The total current significantly hinges on the off-diagonal couplings linking the two energy levels. In addition, the off-diagonal coupling is position-dependent. In the lower panel of Fig. 4, we plot the averaged off-diagonal coupling between the two levels. We compute the mean y -value for each trajectory upon entering the circular limit, followed by an averaging procedure across all trajectories. To accentuate distinctions among various couplings, we subsequently squared the resultant values. Notice that increasing the bias can decrease the off-diagonal coupling, which can result in a decrease in the total electron current. In other words, the voltage bias affects the nuclear distribution, which decreases the off-diagonal coupling between two levels. Upon introducing external driving, the off-diagonal coupling's propensity to decrease with bias weakens, thereby mitigating the prominence of the negative resistance phenomenon.

In Fig. 5, we plot the total electron current as a function of the driving frequency. Here, we are operating within the strong LMI regime ($A = 5$). When the bias is small, the current decreases with the driving frequency. For a larger bias, we see a turnover of the current as a function of driving frequency, i.e., there is an optimal frequency that maximizes the electronic current. That being said, the position of the optimal frequency highly depends on the voltage bias and driving amplitude.

CONCLUSIONS

In summary, we have investigated the effects of the photoinduced Lorentz-like force on molecular motion in quantum transport. Our method is based on the Floquet electronic friction model, with the nonadiabatic dynamics of the coupled light and electronic motion being incorporated into a friction force and random force. We show that the anti-symmetric Lorentz force can redistribute the nuclear motion in the long time limit (cycle limit). In return, the nuclear motion affects electron transport strenuously. In particular, we observe that external driving can enhance and/or reduce electron current under different conditions. Such that there is an optimal driving frequency that maximizes the electron current.

Finally, we recall that Teh *et al.* recently reported SOC

can also give rise to a Lorenz-like Berry force, and such a Berry force on nuclear motion amplifies the spin polarization of the electronic current significantly [11, 14]. Looking forward, we aim to investigate how LMIs affect the SOC induced Berry force. How do the LMIs affect the spin current? Can we use light to control chiral induced spin selectivity? This work is ongoing.

ACKNOWLEDGEMENTS

We thank useful discussions with Hung-Hsuan Teh. W.L. thanks Zhixiang Dai and Siteng Ma for their help in the GPU calculation. We acknowledge the startup funding from Westlake University and the support of the high-performance computing center of Westlake University.

-
- * Electronic address: douwenjie@westlake.edu.cn
- [1] A. W. Jasper, C. Zhu, S. Nangia, and D. G. Truhlar, *Faraday Discussions* **127**, 1 (2004).
 - [2] A. M. Wodtke*, J. C. Tully, and D. J. Auerbach, *International Reviews in Physical Chemistry* **23**, 513 (2004).
 - [3] D. R. Yarkony, *Chemical reviews* **112**, 481 (2012).
 - [4] M. Head-Gordon and J. C. Tully, *The Journal of chemical physics* **103**, 10137 (1995).
 - [5] W. Dou and J. E. Subotnik, *The Journal of Chemical Physics* **148**, 230901 (2018).
 - [6] W. Dou, G. Miao, and J. E. Subotnik, *Physical Review Letters* **119**, 046001 (2017).
 - [7] W. Dou and J. E. Subotnik, *Physical Review B* **96**, 104305 (2017).
 - [8] W. Dou and J. E. Subotnik, *Physical Review B* **97**, 064303 (2018).
 - [9] R. J. Maurer, B. Jiang, H. Guo, and J. C. Tully, *Physical review letters* **118**, 256001 (2017).
 - [10] N. Bode, S. V. Kusminskiy, R. Egger, and F. von Oppen, *Beilstein Journal of Nanotechnology* **3**, 144 (2012).
 - [11] H.-H. Teh, W. Dou, and J. E. Subotnik, *Physical Review B* **104**, L201409 (2021).
 - [12] J.-T. Lu, M. Brandbyge, and P. Hedegård, *Nano letters* **10**, 1657 (2010).
 - [13] J. Subotnik, G. Miao, N. Bellonzi, H.-H. Teh, and W. Dou, *The Journal of Chemical Physics* **151**, 074113 (2019).
 - [14] H.-H. Teh, W. Dou, and J. E. Subotnik, *Physical Review B* **106**, 184302 (2022).
 - [15] V. Mosallanejad, J. Chen, and W. Dou, *Physical Review B* **107**, 184314 (2023).
 - [16] E. Yamaka and K. Sawamoto, *Physical Review* **101**, 565 (1956).
 - [17] T. Oka and H. Aoki, *Physical Review B* **79**, 081406 (2009).
 - [18] T. Kitagawa, T. Oka, A. Brataas, L. Fu, and E. Demler, *Physical Review B* **84**, 235108 (2011).
 - [19] C.-K. Chan, P. A. Lee, K. S. Burch, J. H. Han, and Y. Ran, *Physical review letters* **116**, 026805 (2016).

- [20] J.-i. Inoue and A. Tanaka, *Physical review letters* **105**, 017401 (2010).
- [21] M. Sukharev and A. Nitzan, *Journal of Physics: Condensed Matter* **29**, 443003 (2017).
- [22] T. W. Ebbesen, *Accounts of chemical research* **49**, 2403 (2016).
- [23] M. Hertzog, M. Wang, J. Mony, and K. Börjesson, *Chemical Society Reviews* **48**, 937 (2019).
- [24] L. A. Martínez-Martínez, R. F. Ribeiro, J. Campos-González-Angulo, and J. Yuen-Zhou, *ACS Photonics* **5**, 167 (2018).
- [25] F. Bernardi, M. Olivucci, and M. A. Robb, *Chemical Society Reviews* **25**, 321 (1996).
- [26] J. George, S. Wang, T. Chervy, A. Canaguier-Durand, G. Schaeffer, J.-M. Lehn, J. A. Hutchison, C. Genet, and T. W. Ebbesen, *Faraday discussions* **178**, 281 (2015).
- [27] W. Dou, A. Nitzan, and J. E. Subotnik, *The Journal of chemical physics* **143**, 054103 (2015).
- [28] S. Kohler, J. Lehmann, and P. Hänggi, *Physics Reports* **406**, 379 (2005).
- [29] H. Haug, A.-P. Jauho, et al., *Quantum kinetics in transport and optics of semiconductors*, vol. 2 (Springer, 2008).
- [30] Y. Meir and N. S. Wingreen, *Physical review letters* **68**, 2512 (1992).

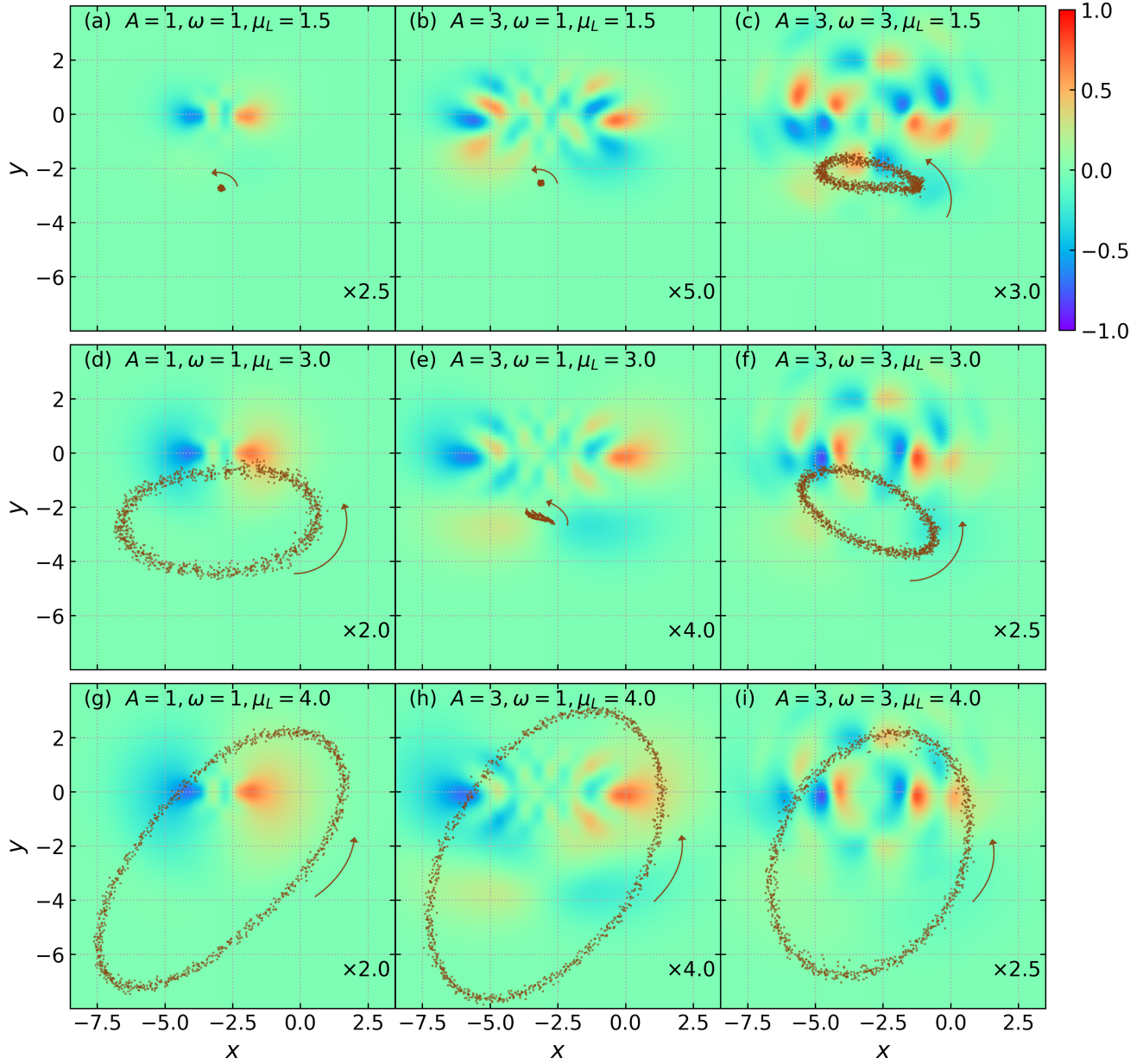


FIG. 2: Anti-symmetric friction tensors in the presence of different driving and voltage bias and the corresponding stabilized trajectory of the nucleus without the fluctuating force. Parameters: $kT = 0.5$, $\Delta = 3$, $\mu_L = -\mu_R$, $\tilde{\Gamma} = 1$, $\lambda_x = 3$, and $\lambda_y = 2$. We select the Floquet level $N = 5$ to ensure convergence. Note that the center of the potential is $(-\lambda_x, -\lambda_y)$, which is also the corresponding center of all the trajectories.

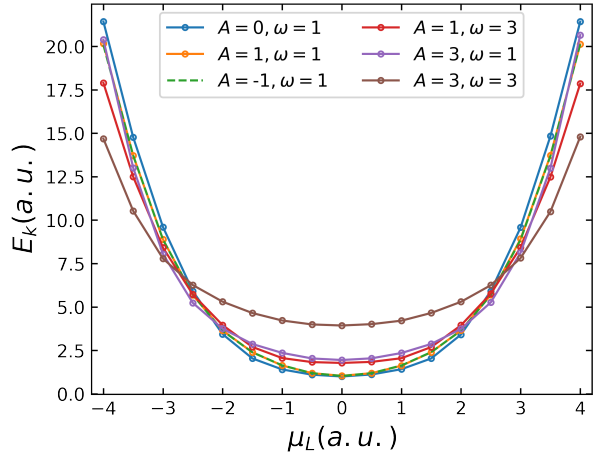


FIG. 3: Kinetic energy under different voltage bias and driving (we change the amplitude and the frequency). Parameters are the same as in FIG. 2. The final kinetic energy value is not stable but always oscillates. We take the average value in the last steps of one single trajectory and the average value of 10,000 trajectories at the same moment. Parameters: $kT = 0.5$, $\Delta = 3$, $\mu_L = -\mu_R$, $\tilde{\Gamma} = 1$, $\lambda_x = 3$, and $\lambda_y = 2$.

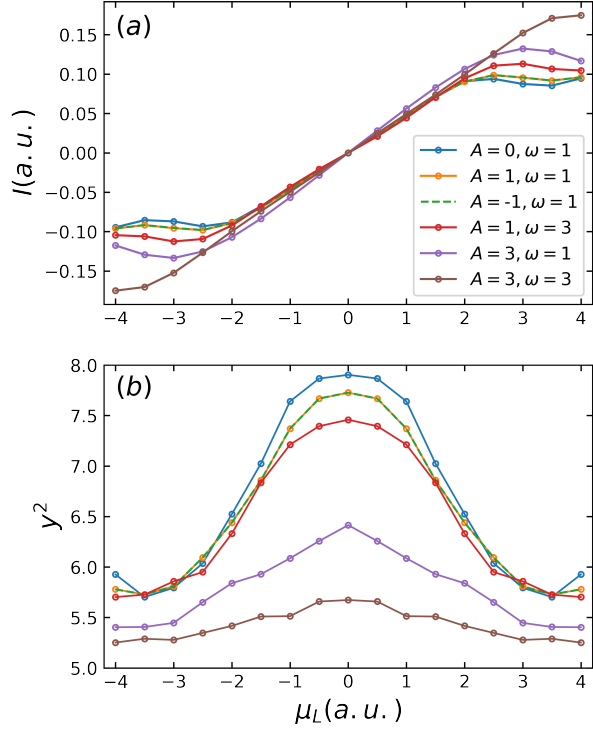


FIG. 4: Localized current under different bias and driving (we change the amplitude and the frequency).

Parameters are the same as in FIG. 2. In fact, the localized current is a function of position; the particles are not static but rotate periodically under the action of the Lorentz-like force in the end, so the current oscillates periodically. Parameters: $kT = 0.5$, $\Delta = 3$, $\mu_L = -\mu_R$, $\tilde{\Gamma} = 1$, $\lambda_x = 3$, and $\lambda_y = 2$.

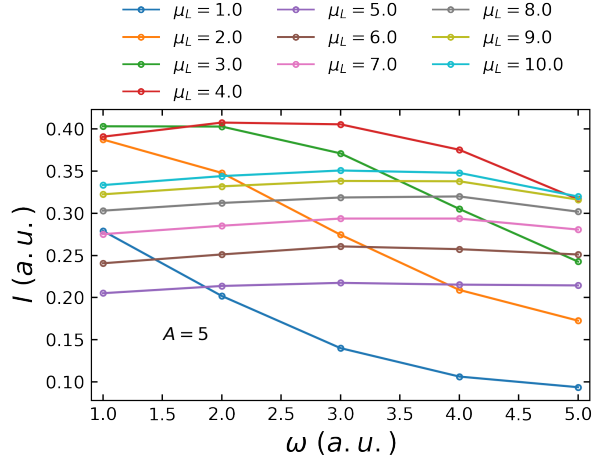


FIG. 5: Relationship between electron current magnitude and light frequency in strong LMI regime $A = 5$. Parameters: $kT = 0.5$, $\Delta = 3$, $\mu_L = -\mu_R$, $\tilde{\Gamma} = 1$, $\lambda_x = 3$, and $\lambda_y = 2$.